This is the accepted manuscript version of the contribution published as:

Ceballos-Escalera, A., Pous, N., **Korth, B., Harnisch, F.**, Balaguer, M.D., Puig, S. (2024): Ex-situ electrochemical characterisation of fixed-bed denitrification biocathodes: A promising strategy to improve bioelectrochemical denitrification *Chemosphere* **347**, art. 140699

The publisher's version is available at:

https://doi.org/10.1016/j.chemosphere.2023.140699

Ex-situ electrochemical characterisation of fixed-bed denitrification biocathodes: a promising strategy to improve bioelectrochemical denitrification

Alba Ceballos-Escalera¹, Narcís Pous¹, Benjamin Korth², Falk Harnisch², M. Dolors Balaguer¹ and Sebastià Puig^{1*}

¹ LEQUIA, Institute of the Environment, University of Girona, c/ Maria Aurèlia Capmany, 69, E-17003, Girona, Spain

² Department of Environmental Microbiology, Helmholtz Centre for Environmental Research GmbH - UFZ, Permoserstraße 15, 04318 Leipzig, Germany

* Corresponding author:

E-mail address: sebastia.puig@udg.edu (S. Puig)

LEQUIA, Institute of the Environment, University of Girona, C/ Maria Aurèlia Capmany, 69, E-17003, Girona, Spain

Tel: +34972418182; Fax: +34972418150

Abstract:

The worldwide issue of nitrate-contaminated groundwater requires practical solutions, and electro-bioremediation offers a promising and sustainable treatment. While it has shown potential benefits, there is room for improvement in treatment rates, which is crucial for its further and effective implementation. In this field, electrochemical characterisation is a valuable tool for providing the foundation for optimising bioelectrochemical reactors, but applying it in fixed-bed reactors is challenging due to its high intrinsic electrical resistance. To overcome these challenges, this study employed the easy and swift eClamp methodology to screen different process parameters and their influence on the performance of fixed-bed denitrifying biocathodes composed of granular graphite. Granules were extracted and studied ex-situ under controlled conditions while varying key operational parameters (such as pH, temperature, and nitrate concentration). In the studied biocathode, the extracellular electron transfer associated with denitrification was identified as the primary limiting step with a formal potential of -0.225 ± 0.007 V vs. Ag/AgCl sat. KCl at pH 7 and 25 °C. By varying the nitrate concentration, it was revealed that the biocathode exhibits a strong affinity for nitrate ($K_{\rm M}^{\rm app}$ of 0.7 ± 0.2 mg N-NO₃⁻ L⁻ 1). The maximum denitrification rate was observed at a pH of 6 and a temperature of 35 $^{\circ}$ C. Furthermore, the findings highlight a 2e⁻/1H⁺ transfer, which holds considerable implications for the energy metabolism of bioelectrochemical denitrifiers. These compiled results provide valuable insights into the understanding of denitrifying biocathodes and enable the improvement and prediction of their performance.

Keywords: Nitrate reduction; cyclic voltammetry; fixed-bed reactor; microbial electrochemical technology; electroactive microorganisms; extracellular electron transfer

1.INTRODUCTION

Electro-bioremediation of nitrate-polluted groundwater is a key application of microbial electrochemical technologies (MET) by using a solid electrode as an electron donor. It has the potential to outcompete conventional treatment approaches by avoiding the addition of chemicals, the production of concentrated brine and the generation of hazardous end-products (Pous et al., 2018; Wang et al., 2020). This water treatment has competitive energy consumption (0.15 kWh $m_{treated}^{-3}$) (Pous et al., 2017) compared to reverse osmosis and electrodialysis (0.3-2.06 kWh $m_{treated}^{-3}$) (Aliaskari and Schäfer, 2021; Twomey et al., 2010). However, conventional treatments still have higher treatment capacities and shorter hydraulic retention times in the range of seconds to minutes (Xu et al., 2018). So far, the electro-bioremediation process has a minimum cathodic hydraulic retention time (HRT_{cat}) of 30 min and a maximum nitrate reduction rate of 0.85 kg N-NO₃- m_{NCc}^{-3} d⁻¹ (Pous et al., 2017). Therefore, the transition to real-world applications depends on improving the treatment rate (i.e., denitrification kinetics) while keeping the strong advantageous characteristics of the technology, such as low energy consumption and the effective conversion of nitrate to N₂.

Electro-bioremediation harnesses the capabilities of electroactive microorganisms (EAM) to exchange electrons with a solid electrode through extracellular electron transfer (EET). Specifically, to achieve denitrifying electro-bioremediation, EAMs are utilised by supplying a solid electrode as an unlimited electron donor to reduce nitrogen compounds, known as denitrifying biocathode (Clauwaert et al., 2007; Sevda et al., 2018). In general, denitrification is carried out by denitrifying microorganisms using four reductases (Vilar-Sanz et al., 2018; Zhong et al., 2021) that progressively reduce nitrate (NO₃-) to nitrite (NO₂-), nitric oxide (NO), nitrous oxide (N₂O), and eventually to nitrogen gas (N₂). The metabolism of EAMs is linked to an external electric circuit using different types of extracellular electron transfer (EET). The metabolism of EAMs is linked to an external electric circuit using different types of extracellular electron transfer (EET) (Costa et al., 2018; Lovley, 2008). The kinetics and thermodynamics of EET play a crucial role in determining the overall performance of the electro-bioremediation treatment.

Additionally, the kinetics of biological nitrate reduction and the selectivity of end-products in electro-bioremediation are influenced by temperature and pH (Zhao et al., 2022). Optimal pH values for enzymes involved in nitrate reduction, nitrite reduction, and nitrous oxide reduction are 7.5, 6.5, and 7.0, respectively (Hu et al., 2022; Zhao et al., 2022). However, microbial electrochemical denitrification has been reported to have an optimal pH range from neutral to alkaline conditions (Korth et al., 2022). Temperature also affects denitrification, with negligible activity below 5 °C and increasing activity up to a maximum of around 25-30 °C (Skiba, 2008). Thus, the optimisation of the operational parameters in denitrifying MET presents a complex challenge due to the interplay between denitrification reactions, microbial energy metabolism, and the EET from the cathode occurring across the cell membrane. Furthermore, EET has implications for microbial energy harvest, particularly concerning the electron carriers involved in EET and the electron transport chain (Korth and Harnisch, 2019; Kracke et al., 2015). A wide range of electron carriers is involved in EET with different pH and temperature optima (Paquete et al., 2019). For instance, different cytochromes have an optimum pH range of 3.5 to 9.0 (Gai et al., 1992; Liu et al., 2012). Furthermore, affinity and uptake of nitrate could limit denitrifying biocathodes. Therefore, understanding the influence of operational parameters such as pH, temperature, and nitrate concentration on the performance of denitrifying biocathodes is necessary to optimise nitrate-contaminated groundwater electro-bioremediation.

Studying the electrochemical interactions between the electrode, the microorganisms, and the medium is crucial in understanding EET behaviour and EAM performance. However, this electrochemical characterisation of fixed-bed electrodes formed by granular graphite, commonly used as denitrifying biocathodes due to the low cost and the high surface-to-volume ratio, presents several challenges (Blázquez et al., 2021; Pous et al., 2017; Zeppilli et al., 2022). The high intrinsic electrical resistance of the fixed-bed electrode leads to poor polarisation behaviour and redox potential heterogeneity (Quejigo et al., 2021). Moreover, the diversity of electrode materials and microorganisms involved poses challenges in generalising their performance, underscoring the necessity to analyse and optimise each system individually. To address these challenges, Quejigo et al. (2018) introduced the eClamp for the electrochemical analysis of single granules sampled from running bioelectrochemical fixed-bed reactors. This exsitu methodology enables rapid screening by cyclic voltammetry and chronoamperometry techniques. The presented study developed a methodology utilising the eClamp to provide valuable insights into the dependency of bioelectrochemical denitrifying reactors on factors such as pH, temperature, nitrate concentration, and the presence of denitrification intermediates. Besides, this study adapted this methodology for the first time to gain detailed

kinetic and thermodynamics of granular graphite denitrifying biocathodes, determining the limiting step for complete nitrate reduction into nitrogen gas and obtaining key parameters such as apparent nitrate affinity constant ($K_{\rm M}^{\rm app}$) and maximum nitrate uptake rate ($v_{\rm max}^{\rm app}$). Consequently, the results provide valuable information for a better understanding of denitrifying biocathodes performance as well as anticipating the impact of critical operational parameters on their performance.

2. MATERIALS AND METHODS

2.1. General conditions

Multiple sets of granular graphite were utilised for electrochemical characterisation, with each test conducted in triplicate. The granular graphite used in the study exhibited a heterogeneous geometry, encompassing diameters between 1.50 - 5.00 mm (enViro-cell, Germany). Nevertheless, the granules were considered spherical with an average diameter of 3.25 mm, resulting in a calculated surface area of 3.32×10^{-5} m⁻² per granule to estimate the surface area of the sample.

Please note that the temperature can have an impact on the reference electrode potential. For example, at temperatures of 15, 25, and 35 °C, the redox potentials of the Ag/AgCl sat. KCl electrode are +0.207, +0.197, and +0.187 V vs. SHE at 25 °C, respectively. Unless otherwise stated, all redox potentials are referred to Ag/AgCl sat. KCl 25 °C, which was the reference electrode used in the experimental set-ups. In the results section 3.4, the redox potentials are recalculated to incorporate the influence of temperature on the reference electrode. This adjustment enables the presentation of normalised potentials at 25°C for more precise comparison and analysis.

2.2. Set-up and operation of denitrifying bioelectrochemical system for granule sampling

Graphite granules were sampled from a previously introduced denitrifying bioelectrochemical fixed-bed reactor (Ceballos-Escalera et al., 2021) (Fig. 1A). The reactor was constructed using a PVC tube (diameter of 55 mm and length of 350 mm), with the cathode (inner part) and anode (outer part) compartments filled with granular graphite (diameter 1.5-5 mm, enViro-cell, Germany) to create a fixed-bed electrode reactor with a 50% porosity (or void fraction). The estimated cathode geometric surface was 0.51 m², and the net liquid cathode compartment (NCC) was 0.3 L. A potentiostat (VSP, BioLogic, France) was used to drive complete nitrate reduction to nitrogen gas, with the cathode potential poised at -0.320 V vs. Ag/AgCl sat. KCl (SE

11, Xylem Analytics Germany Sales GmbH & Co. KG Sensortechnik Meinsberg, Germany) (Pous et al., 2015).

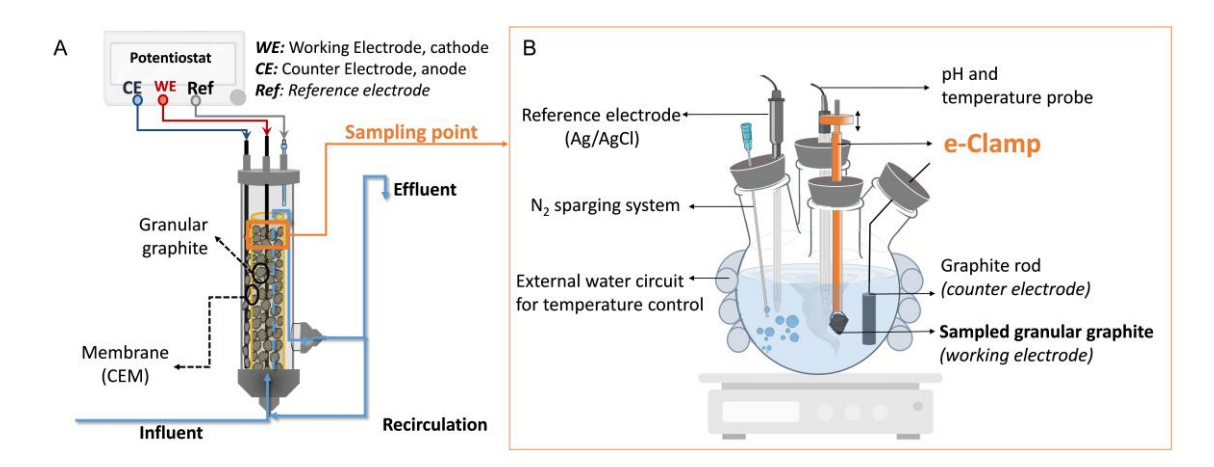


Figure 1: (A) Diagram of the denitrifying bioelectrochemical fixed-bed reactor (Ceballos-Escalera et al., 2021). (B) Illustration of the eClamp set-up used to perform chronoamperometry and cyclic voltammetry experiments with sampled graphite granules.

Throughout the experimental duration, the reactor was continuously fed with synthetic nitrate-containing groundwater (31.3 \pm 5.2 mg N-NO₃⁻ L⁻¹, 1.0 \pm 0.3 mS cm⁻¹, and pH of 7.2 \pm 0.3) at an HRT_{cat} of 2.1 \pm 0.1 h. The reactor was operated at a controlled room temperature of 25 \pm 1 °C. The microbiome on the biocathode was dominated by *Sideroxydans lithotrophicus* sp. (70-50%) with minor contributions of *Denitratisoma oestradiolicum* sp. (5-4%) and *Achromobacter agilis* sp. (4-2%) (Table S1, Supplementary data) (Ceballos-Escalera et al., 2021).

2.3. Granule sampling and *eClamp* set-up

Electrochemical analysis of the sampled granules was carried out using an adapted version of the eClamp (Fig. 1B), first introduced by Quejigo et al. (2018) and later modified by Korth et al. (2022). The eClamp comprised four spring steel wires (1.4310, Febrotec GmbH, Germany) arranged to form a mechanically movable gripper encased by a PEEK tube. The eClamp was used to collect 3 to 5 granules (dry weight of 247 ± 73 mg, estimated surface $1.38 \pm 0.28 \times 10^{-4}$ m²) from the upper part of the cathode compartment of the bioelectrochemical fixed-bed reactor. Immediately after sampling, the collected granules were transferred to a four-necked round bottom flask (Lenz Laborglas GmbH & CO.KG, Germany) containing 300 mL of fresh medium (Fig. 1B). The eClamp served as the working electrode, while the counter electrode was a graphite rod (diameter 10 mm, length 50 mm, Mersen Ibéria, Spain). The set-up was completed with an Ag/AgCl sat. KCl reference electrode (SE 11, Xylem Analytics Germany Sales GmbH & Co. KG Sensortechnik Meinsberg, Germany). A pH and temperature probe (Multimeter

44, Crison, Spain) was installed to continuously monitor both parameters. The pH was manually adjusted by adding either HCl (0.25 M) or NaOH (0.25 M) directly to the medium. The temperature was controlled by using an external heating circuit around the round-bottom flask. A magnetic stirrer was used at 120 rpm to avoid diffusion limitation, and N_2 was continuously sparged to ensure an anoxic condition.

After electrochemical analysis, the granules were dried at room temperature for more than 48 h before determining the dry weight. Assuming that the granules were spheres with an average diameter of 3.25 mm, the surface per granule was estimated at 3.32×10^{-5} m².

2.4. Buffered and non-buffered synthetic groundwater composition

Two types of media were used in this study. Firstly, a buffered synthetic groundwater solution was employed to ensure optimal conditions, including stable pH and higher buffer capacity, for the initial electrochemical characterisation of the different terminal electron acceptors (TEAs) (section 2.5.1). The buffered synthetic groundwater solution comprised 1.05 g L⁻¹ NaHCO₃ as an inorganic carbon source, 1.07 g L⁻¹ KH₂PO₄, 0.16 g L⁻¹ Na₂HPO₄, 0.25 g L⁻¹ NaCl, 0.1 g L⁻¹ MgSO₄×7H₂O, 0.01 g L⁻¹ NH₄Cl and 0.1 mL L⁻¹ of a trace minerals solution (Balch et al., 1979), resulting in an initial pH of 7.0. Secondly, non-buffered synthetic groundwater was used to mimic potential real-world scenarios (variable NO₃⁻¹ concentration, pH, and temperature), when electrochemical characterisation was performed to explore the effect of different operational parameters (sections 2.5.2 and 2.5.3). The non-buffered synthetic groundwater solution contained 0.42 g L⁻¹ NaHCO₃ as an inorganic carbon source, 0.08 g L⁻¹ KH₂PO₄, 0.02 g L⁻¹ Na₂HPO₄, 0.1 g L⁻¹ NaCl, 0.75 g L⁻¹ MgSO₄×7H₂O, 0.01 g L⁻¹ NH₄Cl and 0.1 mL L⁻¹ of the trace minerals solution (Ceballos-Escalera et al., 2021), the resulting pH was 7.2 ± 0.3.

The TEA was added to the medium separately based on the specific test, as outlined below. Three TEAs were used: (i) $NaNO_3$ solution (33,000 mg $N-NO_3^ L^{-1}$) was added for nitrate, (ii) $NaNO_2$ solution (33,000 mg $N-NO_2^ L^{-1}$) was added for nitrite, and (iii) the same medium (buffered synthetic groundwater) saturated with nitrous oxide (previously sparged with nitrous oxide: nitrogen gas, 20:80, Air Liquide, Spain) was added for nitrous oxide. The pH was adjusted using NaOH or HCl (0.25 M).

2.5. Electrochemical characterisation

2.5.1. Utilisation of various terminal electron acceptors: nitrate, nitrite, and nitrous oxide.

The electrochemical characterisation of the granular graphite from the denitrifying fixed-bed biocathode was carried out using different nitrogen species representing TEAs: nitrate, nitrite, nitrous oxide, and their combination. Immediately after sampling, the eClamp was immersed in the buffered synthetic groundwater without TEA (i.e., non-turnover conditions) and chronoamperometry (CA) was performed at -0.320 V (i.e., the same cathode potential of the running reactor). Once the current stabilised (< 5% variation for at least 15 min), three cyclic voltammetry (CV) cycles were executed in a potential range from -0.80 to +0.00 V at a scan rate of 1 mV s⁻¹. Following completion of the CV, CA was repeated under the same conditions. Next, various TEAs were sequentially added, and CA and CV were performed: (i) nitrate; (ii) nitrate and nitrite; (iii) nitrate, nitrite, and nitrous oxide; (iv) nitrite; (v) nitrite and nitrous oxide; (vi) nitrous oxide; and (vii) nitrous oxide and nitrate. Each TEA was added at a final concentration of 33 mg N L⁻¹, which is the same concentration as the influent of the reactor. The buffered synthetic groundwater solution was replaced after steps (iii) and (v) to remove the TEA, which were not required for a particular experiment. Furthermore, abiotic controls were carried out using non-inoculated granular graphite in the buffered synthetic groundwater solution containing nitrate.

2.5.2. Relationship between cathodic current and nitrate concentrations

The electrochemical response of sampled granules to nitrate availability as the TEA was evaluated during CA at -0.320 V, the pH set at 7 and the temperature at 25 °C. Initially, the graphite granules arranged in the eClamp were immersed in a non-buffered synthetic groundwater solution without TEA for 12 h to ensure non-turnover conditions. The concentration of nitrate was then gradually increased from 0 to 50 mg N-NO₃⁻ L⁻¹ by sequentially adding a nitrate-concentrated solution (33,000 mg N-NO₃⁻ L⁻¹) until the current density reached a stable value (< 5% variation for at least 15 min) at each step.

2.5.3. Influence of pH and temperature

The influences of pH and temperature were assessed by (i) recording current during CA at - 0.320 V and (ii) determining the formal potential using CV.

Directly after sampling, the eClamp was submerged into the non-buffered synthetic groundwater solution with nitrate (i.e., turnover condition, 33 mg $N-NO_3^-L^{-1}$) for CA. The pH

analysis was conducted at $25\,^{\circ}$ C and started at a pH of 7. The pH was decreased to 6 by adding HCl (0.25 M), and step-wise increased to 10 using NaOH (0.25 M) by pH steps of 0.5. Every pH step was conducted for a maximum of 30 min or less to reach a stable current density (< 5% variation for at least 15 min). The temperature was varied at a constant pH of 7 starting at 15 °C and gradually increased to 35 °C in 5 °C steps.

For CV analysis, different granules were sampled. The eClamp with the sampled granules was immersed in a non-buffered synthetic groundwater solution with nitrate as TEA (turnover conditions, 33 mg N-NO $_3^-$ L⁻¹) and CA at -0.320 V was performed until current density stabilised (< 5% variation for at least 15 min). The pH effect was evaluated in the potential range from -0.700 to +0.100 V (scan rate: 1 mV s⁻¹) at pH 6, 7, and 8, keeping the temperature at 25 °C. The temperature effect was assessed in the potential range from -0.600 to +0.200 V (scan rate: 1 mV s⁻¹) at 15, 25, and 35 °C, keeping the pH at 7. The potential ranges on CVs were modified due to expecting a variation of the formal potential in the different conditions tested.

2.6. Chemical analysis

Periodic samples of effluent and influent were taken from the denitrifying bioelectrochemical fixed-bed reactor and analysed according to APHA standard water measurements for nitrate, nitrite and ammonium by ionic chromatography (ICS 5000, Dionex, USA) (APHA, 2005) with a detection limit of 0.01 mg-N L⁻¹. Nitrous oxide was measured *in-situ* using an N₂O liquid-phase microsensor (Unisense, Denmark).

2.7. Calculations

The recorded currents from CA and CV were normalised using the dry weight and surface of sampled granular graphite for obtaining the gravimetric current density (j_g , mA g^{-1} and A m^{-2}). Specifically, the j_g (A m^{-2}) was used to calculate the theoretical maximum nitrate reduction rate, assuming a coulombic efficiency (CE) of 100% and the complete conversion of nitrate to nitrogen gas (requiring 5 electrons) (Equation S1, Supplementary data) (Ceballos-Escalera et al., 2021). In addition, the j_g under different nitrate concentrations were used to calculate the nitrate affinity constant (K_M^{app}) and maximum nitrate uptake rate (v_{max}^{app}) by applying adapted Michaelis-Menten kinetic (Equation S2, Supplementary data) and using the Curve fitting tool from MATLAB software. Please note that determined values for K_M^{app} and v_{max}^{app} represent apparent Michaelis-Menten constants that are subject to radial diffusion, substrate depletion, properties of the biocathode such as thickness and density, and convection. The CV data analysis was performed by SOAS using the third cycle representing steady-state (Fourmond et

al., 2009). Formal potentials (E^f) were calculated as the mean value of the oxidative (E_{ox}) and reductive (E_{red}) peaks potentials of the 1st derivative of the current signal. Finally, the Nernst equation was used to evaluate the results obtained from the electrochemical characterisation (Equation S3, Supplementary data). This equation provides insight into the theoretical influence of certain parameters (e.g., temperature, pH and electron involvement) on the redox potential.

The results were subjected to different statistical tests by applying Microsoft Excel. Analysis of variance (t-student and ANOVA) was performed assuming a normal distribution, two-sided analysis, heteroscedasticity, and a 95% confidence level. The linearity of the results was determined by linear regression, determining the coefficient of determination (R^2) and the Pearson correlation coefficient (r_{xy}).

3. RESULTS AND DISCUSSION

3.1. Performance of the denitrifying bioelectrochemical fixed-bed reactor

This study focuses on the *ex-situ* electrochemical characterisation of a bioelectrochemical fixed-bed reactor treating synthetic nitrate-contaminated groundwater. During the study, a small fraction of granular graphite constituting the biocathode, equivalent to approximately 0.5% (around 75 granules), was extracted without interrupting reactor operation. This quantity of granules is considered to be representative of the reactor, as it is consistent with other experiments where granular graphite was extracted for *ex-situ* characterisation within the range of 0.1 to 0.5% (Korth et al., 2022; Quejigo et al., 2021).

Throughout the analysis, the reactor was operated continuously at cathodic hydraulic retention time (HRT_{cat}) of 2.1 ± 0.1 h, while the nitrate removal was maintained at 0.29 ± 0.08 kg N-NO₃⁻ m⁻³_{NCC} d⁻¹ (0.17 ± 0.05 g N-NO₃⁻ m⁻² d⁻¹). Nitrate reduction efficiency was $82 \pm 13\%$, resulting in an effluent nitrate concentration of 6.6 ± 3.4 mg N-NO₃⁻ L⁻¹. The pH in the effluent was 7.3 ± 0.3 , and the electric conductivity was 1.0 ± 0.3 mS cm⁻¹. These results are consistent with those observed during the previous operation before granule extraction (nitrate removal from 0.17 to 0.52 kg N-NO₃⁻ m⁻³_{NCC} d⁻¹, effluent pH of 8.0 ± 0.3) (Ceballos-Escalera et al., 2021). The reactor demonstrated a substantial capacity for reducing nitrate to nitrogen gas with high selectivity (>99%). Throughout the operational period, nitrate reduction intermediates did not accumulate in the effluent, neither nitrite (0.06 ± 0.05 mg N-NO₂⁻ L⁻¹) nor nitrous oxide (not detected). Simultaneously, the possibility of dissimilatory nitrate reduction to ammonium was excluded because ammonium was not detected in the effluent either (<0.01 mg N-NH₄⁺ L⁻¹). Furthermore, the cathodic coulombic efficiency of $87 \pm 14\%$, assuming denitrification using the cathode as an

electron donor, supported this primary pathway for nitrate reduction. In addition, the contribution of hydrogen-mediated denitrification was considered marginal, as the cathode working potential of -0.320 V was well above the -0.700 V threshold previously shown to be necessary for sustained bioelectrochemical hydrogen production (Batlle-Vilanova et al., 2014).

3.2. Fundamental electrochemical characterisation: formal potential and gravimetric current density

The eClamp was used to perform CV analysis with sampled graphite granules in the presence of nitrate and intermediates (nitrite and nitrous oxide) of the denitrification pathway as terminal electron acceptors (TEAs). The increase in gravimetric current density (j_q) of biotic compared to abiotic non-turnover CVs and the change in the voltammogram shape towards a catalytic wave under turnover conditions demonstrated the activity of a denitrifying electroactive microbiome at the sampled granules (Fig. 2A). The significant increase in j_g during CA at -0.320 V compared to the negligible jg observed during non-turnover (Fig. 2B), clearly connects the electroactive response to the reduction of nitrogen species, excluding a role for hydrogen-mediated denitrification which is only observed during more negative cathode potentials (Batlle-Vilanova et al., 2014). In parallel, performing CV in the presence of different TEAs (Fig. S1, Supplementary data) led to the determination of only one single formal potential ($\it E^{f}$) at -0.225 \pm 0.007 V. Having only one single E^{f} that was identical for nitrate and different intermediates of the denitrification pathway (nitrite, nitrous oxide, or a combination thereof) (Fig. 2A, Fig. S1, Table S2) as TEA, points to one common limiting step. It also highlights that the entire denitrification pathway can be effectively managed by controlling the cathode at one single potential. Presumably, this is the electron uptake by the EAMs from the graphite granules. However, the poor electric conductivity of granular graphite and the resulting limited signal resolution could have prevented a detailed analysis of further, maybe even underlying, redox peaks. Furthermore, the electrode material may also influence the limiting step. For instance, denitrifying biocathode using carbon paper as the electrode material revealed the intracellular catalytic reaction as the primary limiting step, while nitrate supply and electron shuttle transfer can also act as limiting steps in other scenarios (Wang and Zhang, 2019).

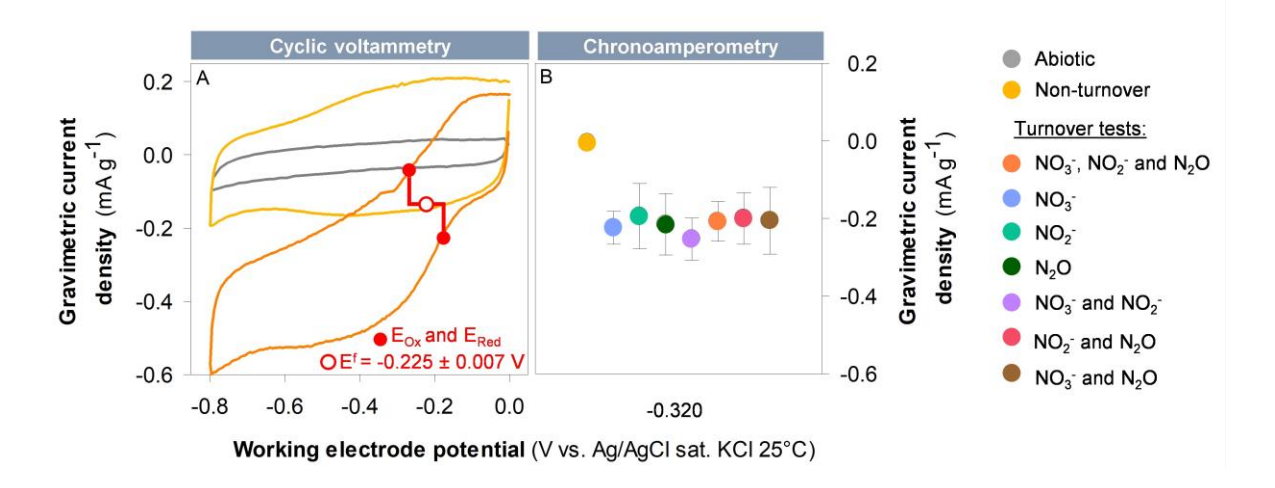


Figure 2: (A) Representative voltammograms of granular graphite under abiotic, biotic non-turnover and turnover conditions at pH 7 and 25 °C. (B) Average gravimetric current densities during chronoamperometry at -0.320 V vs. Ag/AgCl sat. KCl 25°C in non-turnover and in the presence of nitrate and different denitrification intermediates. Representative voltammograms of all combinations of terminal electron acceptors and electrochemical data are depicted in Fig. S1 and Table S2. n = 3.

Denitrifying biocathodes were already electrochemically characterised several times, but the *E*^f determined here considerably deviates from reported literature values. For instance, Pous et al. (2014) showed two formal potentials at -0.300 V and -0.700 V (pH 8.0), in the case of a biocathode mainly formed by *Thiobacillus* spp., corresponding to nitrate and nitrite reduction, respectively. Similar results were reported for a biofilm formed by *Pseudomonas*, *Natronococcus*, and *Pseudoalteromonas* spp. with two formal potentials at -0.294 V and -0.724 V (pH 9.5) (Chaudhary et al., 2021). Other studies reported electroactive redox sites at -0.374 V (pH 7.0) for a denitrifying biofilm mainly consisting of *Geobacter* (Pous et al., 2016), or -0.487 V and -0.406 V (pH 7.0) in the case of a microbiome composed of *Pseudomonas nitroreducens* and *Paracoccus versutus* (Korth et al., 2022). Hence, these observations indicate a certain variability in the microbial composition and thermodynamics of denitrifying biocathodes. Consequently, deriving general statements on denitrifying biocathodes and their performance is challenging, and the characterisation of individual biocathodes is necessary to provide key information for optimising their performance.

The main microorganism within the studied denitrifying biocathode was likely *Sideroxydans lithotrophicus* sp., as previously analysed (Table S1, Supplementary data) (Ceballos-Escalera et al., 2021). It possesses a three-gene cluster encoding homologs of redox proteins of *Shewanella oneidensis* MR-1 and is assumed to conduct EET through a porin-cytochrome MtoAB complex on the outer membrane (Zhao et al., 2021). MtoA (decaheme c-type cytochrome) exhibits

reversible electrochemical redox behaviour within the range of -0.200 to -0.500 V (pH 7.1, scan rate of 50 mV s⁻¹) (Liu et al., 2012), which is consistent with the E^f determined here (-0.225 \pm 0.007 V). In terms of the potential microbial energy gain, it seems that microorganisms are currently unable to effectively harness energy between the electrode potential and the redox potential (E^f) of the electron carrier involved in EET (Korth and Harnisch, 2019; Kracke et al., 2015; Rosenbaum et al., 2011). While there is supporting evidence for this hypothesis in anodic reactions, our understanding of electron uptake from a cathode remains limited. Furthermore, assuming that the determined E^f of -0.225 \pm 0.007 V represents the electron-accepting redox centre, the energy loss to run the fixed-bed reactor and to drive bioelectrochemical denitrification amounts to 0.095 V at a cathode potential of -0.320 V. Minimising energy losses in operational reactors is vital for optimising their energy consumption, although it is also important to consider the impact of the cathodic potential and the resulting differences in kinetics.

The reduction kinetics of the single granules were evaluated during CA at -0.320 V. Granular graphite extracted from the running reactor only showed relevant reduction currents during turnover conditions, leading to the conclusion that there was a direct relation between the $j_{
m g}$ and denitrification reactions (Fig. 2B). Thereby j_g averaged to -0.21 \pm 0.06 mA g^{-1} (-0.34 \pm 0.10 A m^{-2}) considering different turnover conditions (including j_g in the presence of nitrate, nitrite, nitrous oxide, and a combination thereof, Table S2). A relatively high standard deviation of around 30% was observed, which could be ascribed to the heterogeneity of biomass on granules in relation to both microbial composition and biomass quantity, as well as the possibility that the characteristics of the graphite granules may not be uniform. Thus, j_g was independent of the type of TEA (p-value of 0.99). This finding supports the hypothesis that the same EET step limited the overall denitrifying performance, irrespective of the TEA present in the media (nitrate, nitrite, nitrous oxide). This is beneficial for potential applications as it effectively mitigates the accumulation of harmful denitrification intermediates such as nitrite and nitrous oxide. The absence of nitrite and nitrous oxide accumulation in the effluent of the operational reactor, along with the high coulombic efficiency observed (87 ± 14%), provides further evidence supporting the complete reduction from nitrate to nitrogen gas.

Remarkably, a comparable j_g was reported in another study also exposing denitrifying granules to nitrate as TEA (around -0.15 mA g⁻¹) (Korth et al., 2022), indicating the robustness and reliability of the obtained results. Extrapolating the j_g obtained from sampled granules during turnover conditions to the fixed-bed reactor scale and assuming complete denitrification (5 electrons per molecule of nitrate), a maximum nitrate reduction rate to nitrogen gas of 0.85 \pm

0.24 g N-NO₃⁻ m⁻² d⁻¹ (1.41 ± 0.41 kg N-NO₃⁻ m⁻³_{NCC} d⁻¹) in the bioelectrochemical fixed-bed reactor can be estimated (see Equation 1 in Supplementary data). In contrast, the maximum rate observed in the studied reactor was 0.31 g N-NO₃⁻ m⁻² d⁻¹ (0.52 kg N-NO₃⁻ m⁻³_{NCC} d⁻¹) (Ceballos-Escalera et al., 2021). This observation implies that the denitrifying capacity of the operated bioelectrochemical fixed-bed reactor is not fully exploited, and their performance could be improved through process and reactor engineering resembling eClamp conditions at the reactor scale. The eClamp is characterised by an excellent electric connection between granular graphite and the current collector, and it is submerged in fully mixed media, which suppress limitations related to substrate diffusion, such as nitrates and H⁺ (i.e., avoids pH imbalances). Therefore, special attention should be given to the poor polarisation behaviour of the granule bed and its improvement with wide-ranging current collectors (Quejigo et al., 2021). Moreover, a continuous improvement of reactor mixing is required (Pous et al., 2017; Vilà-Rovira et al., 2015) to ensure that nitrate is available all around the biocathode and that pH gradients are mitigated within the cathodic fixed-bed electrode. The following sections demonstrate how nitrate availability, pH, and temperature affect the denitrifying EET.

3.3. Application of Michaelis-Menten kinetics to the denitrifying biocathode

As nitrate is the main TEA, its uptake plays a significant role in the kinetics of a denitrifying biocathode. One approach to quantify this is the Michaelis-Menten equation, which has been applied only a few times to electroactive biofilms so far (Fujii et al., 2021; Hassan et al., 2019; Van Doan et al., 2013). It should be noted that the Michaelis-Menten equation was established for planktonic cell cultures. Thus, the derived parameters, affinity constant ($K_{\rm M}^{\rm app}$) and maximum uptake rate ($v_{\rm max}^{\rm app}$), must be considered as "apparent parameters" as they are influenced by factors such as biofilm thickness, biofilm density, the surface area of granular graphite, and radial diffusion.

Each replicate exhibited typical Michaelis-Menten kinetics ($R^2 > 0.98$) with $v_{\text{max}}^{\text{app}}$ and $K_{\text{M}}^{\text{app}}$ of 0.37 \pm 0.06 mA g⁻¹ and 0.7 \pm 0.2 mg N-NO₃⁻ L⁻¹, respectively, at pH 7 and 25 °C (Fig. 3). This current consumption rate was slightly higher but still significant compared to the turnover tests described in section 3.2 (p-value of <0.01). This indicates that the maximum nitrate removal rate may be even higher than previously predicted, potentially reaching values up to 1.31 \pm 0.37 g N-NO₃⁻ m⁻² d⁻¹ (2.16 \pm 0.62 kg N-NO₃⁻ m⁻³_{NCC} d⁻¹). The reason behind this observation is currently unknown, but the main difference between these experiments lies in the medium composition (non-buffered synthetic groundwater medium vs. buffered synthetic groundwater medium) (Zhang et al., 2019). However, other factors, such as reactor heterogeneity and the impact of subsequent cyclic voltammetry cycles in section 3.2 (Smit et al., 2021), may also contribute to

this difference. In addition, the determined $K_{\rm M}^{\rm app}$ demonstrates a high nitrate affinity of the microbiome attached to the granular graphite. Nitrate affinity can vary depending on the characteristics of the microbial community. For instance, studies with other denitrifying microbiomes have reported $K_{\rm M}^{\rm app}$ values comparable to those found here (0.2 mg N-NO₃- L⁻¹ (Bardon et al., 2016) and 0.2-9.0 mg N-NO₃- L¹ (García-Ruiz et al., 1998)), although these studies were conducted with non-electroactive, planktonic cells. The determined high nitrate affinity ensures that nitrate uptake does not limit reactor operation when nitrate concentrations exceed drinking water standards (NO₃-> 11.3 mg N-NO₃-L⁻¹; European Directive 2020/2184). This applies when the nitrate concentration is homogenous throughout the reactor and the biofilm.

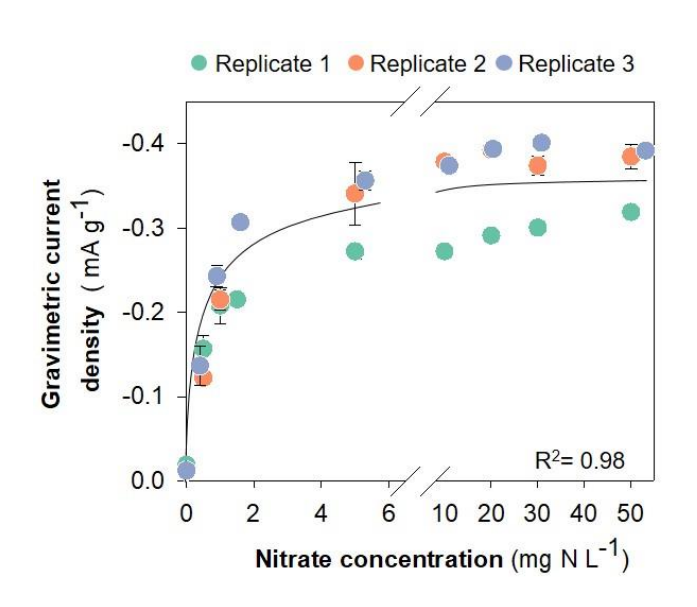


Figure 3. Gravimetric current densities of the sampled granules at different concentrations nitrate during chronoamperometry at -0.320 V vs. Ag/AgCl sat. KCl 25°C, under a constant pH 7 and temperature of 25° C (n = 3). A representative course of the gravimetric current density of one replicate is presented in Fig. S2 in Supplementary data. The black line represents the regression line that takes into account all replicates.

3.4. Electrochemical characterisation under different pHs and temperatures

The pH and temperature are crucial for denitrification and the potential accumulation of intermediates and end products. Typically, biological denitrification has an optimal pH range between 7-8 at mesophilic temperatures (Skiba, 2008). However, denitrification can also proceed at extreme pH and temperatures (e.g., at pH 12 or 3 °C) (Albina et al., 2021; Di Capua et al., 2017). In this study, the electrochemical activity of the denitrifying microbiome attached to sampled granules was evaluated in the pH range of 6 to 10 and temperature range of 15 to 35 °C (Fig. 4). Within these ranges j_g showed a linear response to changes in both pH (r_{xy} = 0.84, R^2 = 0.70) and temperature (r_{xy} = -0.89, R^2 = 0.80), without exhibiting activity maxima or minima. The highest j_g was observed at pH 6 and 35°C, and decreased by 0.07 mA g⁻¹ per pH unit or by 0.01 mA g⁻¹ for every 1 °C decrease in temperature. The results are consistent with the optimal

conditions (pH 6.0-6.5 and 30 °C) for the growth of the dominant microorganism of the biocathode (*Sideroxydans* spp.) (Emerson et al., 2013).

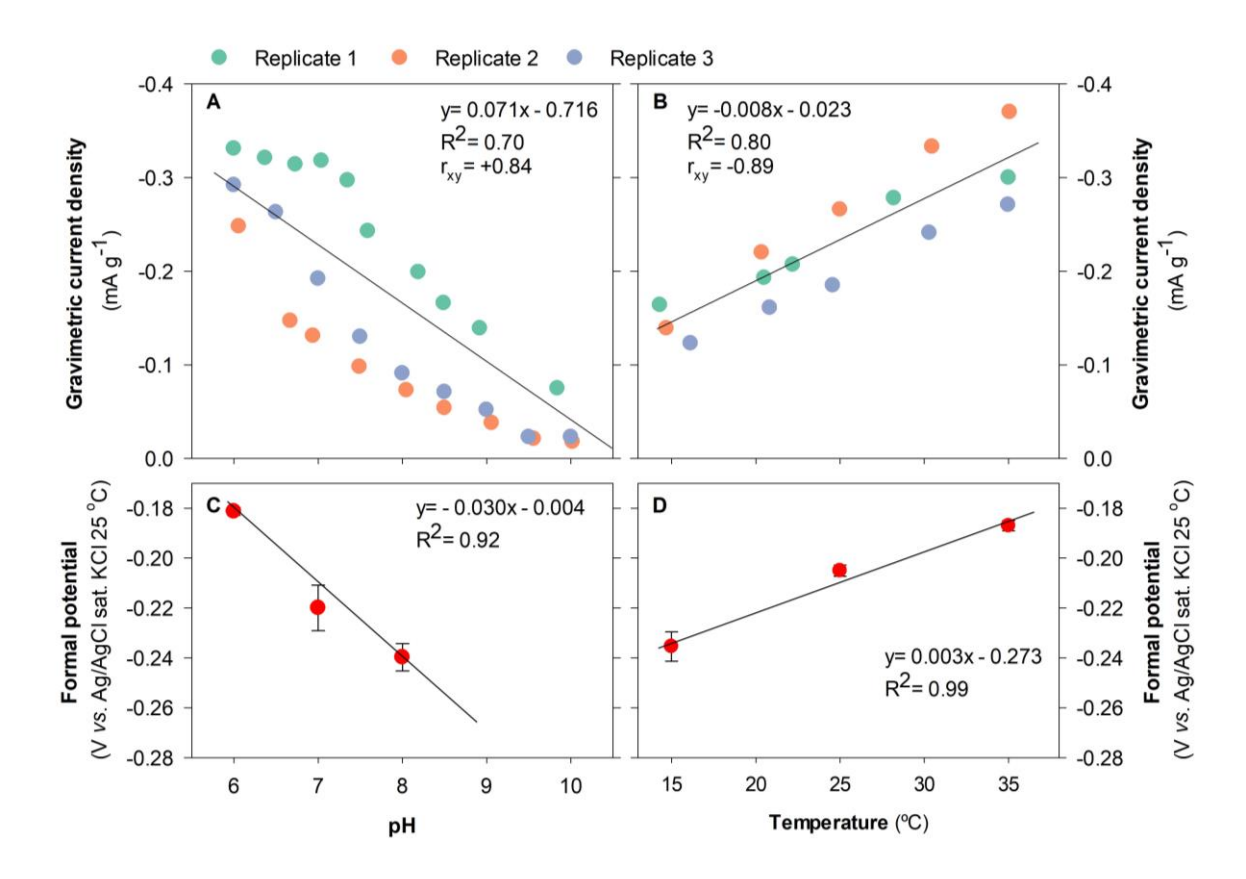


Figure 4. Gravimetric current densities during chronoamperometry at -0.320 V vs. Ag/AgCl sat. KCl 25°C (A and B) and formal potential extracted from cyclic voltammetry (C and D). During the experiments, either pH or temperature varied, while the other parameter was kept constant at 25 °C (A and C) or pH of 7 (B and C). The formal potentials of the denitrifying biocathode at different temperatures (D) are normalised at 25 °C, considering the temperature effect on the reference electrode. Linear regression, the coefficients of determination (R^2) and the Pearson correlation coefficients (r_{xy}) were determined with all the points of the replicates (n=3). Corresponding cyclic voltammograms are presented in Fig. S3 in Supplementary data.

In addition, the parameters pH and temperature had a significant effect on the E^f of the biocathode (*p-value* of < 0.01 by ANOVA for both parameters, Fig. 4C and 4D). E^f became more positive with lower pH (Fig. 4C), exhibiting typical Nernst behaviour. This behaviour was previously demonstrated for electroactive denitrifying biofilms attached to granular graphite (Korth et al., 2022) and is likely related to the redox-Bohr effect on redox centres responsible for EET, which is, so far, fundamentally analysed only for anodic biofilms (Morgado et al., 2012). According to the Nernst equation, an E^f shift of 0.059 $V/\frac{z}{m}$ is expected for a unit of pH, with z being the number of electrons exchanged and m the number of protons. Therefore, the observed E^f shift of 0.030 V per pH unit indicates a coupled $2e^-/1H^+$ transfer (Bard and Faulkner,

2001). Consequently, in addition to the proton being transferred from the extracellular space to the cytosol during EET, an additional proton must be provided intracellularly to balance the charge during the nitrate reduction to nitrite (requiring 2 electrons and 2 protons). Therefore, the intracellular pH and, in turn, the microbial energy harvest at the electron-transport chain are affected by this EET mechanism. On the other hand, the temperature shifts the E^{f} of the biocathode by 0.013 V per 5 °C (Fig. 4D), which is higher than predicted by the Nernst-equation (<0.001 V for every 5 °C for a $2e^{-}/1H^{+}$ transfer). This observation provides evidence of the influence of the temperature on the proteome of the denitrifying biocathode (e.g., by enzyme activity and conformational changes of cytochromes) (Battistuzzi et al., 2001). The positive Ef shift in the studied denitrifying biocathode for higher temperatures and lower pH is beneficial for the microorganisms as the EET rate increases due to the higher potential difference between cathode and redox centres, providing more electrons for higher nitrate reduction rates. More positive E^{f} of redox centres is also expected to decrease the catabolic energy harvest as the potential difference between redox centres and the TEA nitrate becomes smaller. Nevertheless, as the nitrate reduction to nitrite also depends on temperature and pH, according to the Nernst equation, its redox potential also becomes more positive under higher temperature and lower pH, balancing the more positive $E^{\rm f}$.

The established correlations serve as valuable tools for predicting the efficiency of bioelectrochemical denitrification in real-world scenarios, accounting for variables such as variable influent pH or temperature. Besides, these relations between physicochemical parameters and denitrification activity enable the optimisation of reactor performance. For instance, nitrate removal could be increased by 47% by controlling the pH at 6 instead of running the reactor at pH 8.0 ± 0.3 . Similarly, raising the reactor temperature from 25 °C (working temperature) to 35 °C could improve treatment performance by 36%.

4. CONCLUSIONS

This study employed a non-invasive method for comprehensive electrochemical analysis using sampled graphite granules from the biocathode of a denitrifying fixed-bed bioelectrochemical reactor, which was dominated by *Sideroxydans lithotrophicus* sp. as previously shown (Ceballos-Escalera et al., 2021. This methodology now enables the assessment of electrochemical behaviour and the performance of denitrifying fixed-bed bioelectrochemical reactors under controlled conditions (i.e., redox potential, substrate availability, pH, and temperature) without disrupting the running reactor. The denitrifying biocathode exhibited a single limiting step at a formal potential of -0.225 ± 0.007 V vs. Ag/AgCl sat. KCl at pH 7 and 25 °C, independently of the

availability of different TEA involved in the denitrification pathway (nitrate, nitrite, nitrous oxide, or a combination of them). Adapting the Michaelis-Menten kinetic to experiments with different nitrate concentrations revealed a high nitrate affinity, with a $K_{\rm M}^{\rm app}$ of 0.7 \pm 0.2 mg N- $NO_3^- L^{-1}$. This high affinity ensures a maximum high nitrate treatment rate (v_{max}^{app} 0.37 ± 0.06 mA g⁻¹) in the range of nitrate concentrations above drinking water standards (>11.3 mg N-NO₃⁻¹ L-1). Interestingly, extrapolating the gravimetric current density obtained from sampled granules to the reactor level highlighted the potential for denitrification performance to more than double with correct adjustments. The conducted methodology efficiently enabled rapid screening to estimate the performance of denitrifying fixed-bed bioelectrochemical reactors under fluctuating conditions induced by, e.g., climatic conditions and water characteristics. Notably, it revealed a linear dependency between pH and temperature with the gravimetric current density, with the highest activity observed at a pH of 6 and 35°C. The insights into the dependency of bioelectrochemical denitrification on pH, temperature, availability of terminal electron acceptor, and nitrate concentration obtained at granule level will guide the engineering of denitrifying fixed-bed bioelectrochemical reactors for future implementation in water treatment, also providing first guidelines for enhancing treatment rates by manipulating process conditions.

5. Acknowledgements

This work was funded through the European Union's Horizon 2020 project ELECTRA [no. 826244, 2019]. A.C-E. was supported by a PhD grant from the University of Girona (IF_UDG2020) and a mobility grant (IFMOB2021). S.P. is a Serra Hunter Fellow (UdG-AG-575) and acknowledges the funding from the ICREA Academia award. LEQUIA has been recognised as a "consolidated research group" (Ref 2021 SGR01352) by the Catalan Agency of Research and Universities. The authors acknowledge the technical support of Serveis Tècnics de Recerca-Universitat de Girona. This work was supported by the Helmholtz Association in the frame of the Integration Platform "Tapping nature's potential for sustainable production and a healthy environment" at the UFZ.

References

Albina, P., Durban, N., Bertron, A., Albrecht, A., Robinet, J.C., Erable, B., 2021. Nitrate and nitrite bacterial reduction at alkaline pH and high nitrate concentrations, comparison of acetate versus dihydrogen as electron donors. J. Environ. Manage. 280, 111859. https://doi.org/10.1016/j.jenvman.2020.111859

- Aliaskari, M., Schäfer, A.I., 2021. Nitrate, arsenic and fluoride removal by electrodialysis from brackish groundwater. Water Res. 190, 116683. https://doi.org/10.1016/j.watres.2020.116683
- APHA, 2005. Standard Methods for the Examination of Water and Wastewater, 19th ed. Am. Public Heal. Assoc. Washingt. DC, USA.
- Balch, W.E., Fox, G.E., Magrum, L.J., Woese, C.R., Wolfe, R.S., 1979. Methanogens: reevaluation of a unique biological group. Microbiol. Rev. 43, 260–296. https://doi.org/10.1128/mr.43.2.260-296.1979
- Bard, A.J., Faulkner, L.R., 2001. Electrochemical Methods: Fundamentals and Applications, 2nd Edition, Electrochemical Methods Fundamentals and Applications. https://doi.org/https://doi.org/10.1023/A:1021637209564
- Bardon, C., Poly, F., Piola, F., Pancton, M., Comte, G., Meiffren, G., Haichar, F. el Z., 2016. Mechanism of biological denitrification inhibition: procyanidins induce an allosteric transition of the membrane-bound nitrate reductase through membrane alteration. FEMS Microbiol. Ecol. 92, fiw034. https://doi.org/10.1093/FEMSEC/FIW034
- Batlle-Vilanova, P., Puig, S., Gonzalez-Olmos, R., Vilajeliu-Pons, A., Bañeras, L., Balaguer, M.D., Colprim, J., 2014. Assessment of biotic and abiotic graphite cathodes for hydrogen production in microbial electrolysis cells. Int. J. Hydrogen Energy 39, 1294–1305. https://doi.org/10.1016/j.ijhydene.2013.11.017
- Battistuzzi, G., Borsari, M., Sola, M., 2001. Medium and Temperature Effects on the Redox Chemistry of Cytochrome c. Eur. J. Inorg. Chem 2001, 2989–3004. https://doi.org/10.1002/1099-0682
- Blázquez, E., Gabriel, D., Baeza, J.A., Guisasola, A., Ledezma, P., Freguia, S., 2021. Implementation of a sulfide–air fuel cell coupled to a sulfate-reducing biocathode for elemental sulfur recovery. Int. J. Environ. Res. Public Health 18, 5571. https://doi.org/10.3390/ijerph18115571
- Ceballos-Escalera, A., Pous, N., Chiluiza-Ramos, P., Korth, B., Harnisch, F., Bañeras, L., Balaguer, M.D., Puig, S., 2021. Electro-bioremediation of nitrate and arsenite polluted groundwater. Water Res. 190, 116748. https://doi.org/10.1016/j.watres.2020.116748
- Chaudhary, S., Singh, R., Yadav, S., Patil, S.A., 2021. Electrochemical enrichment of haloalkaliphilic nitrate-reducing microbial biofilm at the cathode of bioelectrochemical systems. iScience 24, 102682. https://doi.org/10.1016/j.isci.2021.102682
- Clauwaert, P., Rabaey, K., Aelterman, P., De Schamphelaire, L., Pham, T.H., Boeckx, P., Boon, N., Verstraete, W., 2007. Biological denitrification in microbial fuel cells. Environ. Sci. Technol. 41, 3354–3360. https://doi.org/10.1021/es062580r
- Costa, N.L., Clarke, T.A., Philipp, L.A., Gescher, J., Louro, R.O., Paquete, C.M., 2018. Electron transfer process in microbial electrochemical technologies: The role of cell-surface exposed conductive proteins. Bioresour. Technol. 255, 308–317. https://doi.org/10.1016/J.BIORTECH.2018.01.133
- de Smit, S.M., Buisman, C.J.N., Bitter, J.H., Strik, D.P.B.T.B., 2021. Cyclic Voltammetry is Invasive on Microbial Electrosynthesis. ChemElectroChem 8, 3384–3396. https://doi.org/10.1002/CELC.202100914
- Di Capua, F., Milone, I., Lakaniemi, A.M., Lens, P.N.L., Esposito, G., 2017. High-rate autotrophic denitrification in a fluidized-bed reactor at psychrophilic temperatures. Chem. Eng. J. 313, 591–598. https://doi.org/10.1016/J.CEJ.2016.12.106
- Emerson, D., Field, E.K., Chertkov, O., Davenport, K.W., Goodwin, L., Munk, C., Nolan, M., Woyke, T., 2013. Comparative genomics of freshwater Fe-oxidizing bacteria: implications for physiology, ecology, and systematics. Front. Microbiol. 4, 254. https://doi.org/10.3389/FMICB.2013.00254
- Fourmond, V., Hoke, K., Heering, H.A., Baffert, C., Leroux, F., Bertrand, P., Léger, C., 2009. SOAS: A free program to analyze electrochemical data and other one-dimensional signals. Bioelectrochemistry 76, 141–147. https://doi.org/10.1016/j.bioelechem.2009.02.010
- Fujii, K., Yoshida, N., Miyazaki, K., 2021. Michaelis—Menten equation considering flow velocity reveals how microbial fuel cell fluid design affects electricity recovery from sewage wastewater. Bioelectrochemistry 140, 107821. https://doi.org/10.1016/j.bioelechem.2021.107821
- Gai, M., Yano, T., Tamegai, H., Fukumori, Y., Yamanaka, T., 1992. Thiobacillus ferrooxidans cytochrome c oxidase: Purification, and molecular and enzymatic features. J. Biochem. 112, 816–821. https://doi.org/10.1093/oxfordjournals.jbchem.a123982
- García-Ruiz, R., Pattinson, S.N., Whitton, B.A., 1998. Kinetic parameters of denitrification in a river continuum. Appl. Environ. Microbiol. 64, 2533–2538. https://doi.org/10.1128/aem.64.7.2533-2538.1998
- Hassan, H., Dai, S., Jin, B., 2019. Bioelectrochemical Reaction Kinetics, Mechanisms, and Pathways of

- Chlorophenol Degradation in MFC Using Different Microbial Consortia. ACS Sustain. Chem. Eng. 7, 17263–17272. https://doi.org/10.1021/acssuschemeng.9b04038
- Hu, L., Wang, X., Chen, C., Chen, Jianmeng, Wang, Z., Chen, Jun, Hrynshpan, D., Savitskaya, T., 2022. NosZ gene cloning, reduction performance and structure of Pseudomonas citronellolis WXP-4 nitrous oxide reductase. RSC Adv. 12, 2549. https://doi.org/10.1039/d1ra09008a
- Korth, B., Harnisch, F., 2019. Spotlight on the energy harvest of electroactive microorganisms: The impact of the applied anode potential. Front. Microbiol. 10, 1352. https://doi.org/10.3389/fmicb.2019.01352
- Korth, B., Pous, N., Hönig, R., Haus, P., Corrêa, F.B., Nunes da Rocha, U., Puig, S., Harnisch, F., 2022. Electrochemical and Microbial Dissection of Electrified Biotrickling Filters. Front. Microbiol. 13, 869474. https://doi.org/10.3389/FMICB.2022.869474/BIBTEX
- Kracke, F., Vassilev, I., Krömer, J.O., 2015. Microbial electron transport and energy conservation The foundation for optimizing bioelectrochemical systems. Front. Microbiol. 6, 575. https://doi.org/10.3389/fmicb.2015.00575
- Liu, J., Wang, Z., Belchik, S.M., Edwards, M.J., Liu, C., Kennedy, D.W., Merkley, E.D., Lipton, M.S., Butt, J.N., Richardson, D.J., Zachara, J.M., Fredrickson, J.K., Rosso, K.M., Shi, L., 2012. Identification and characterization of M to A: A decaheme c-type cytochrome of the neutrophilic Fe(II)-oxidizing bacterium Sideroxydans lithotrophicus ES-1. Front. Microbiol. 3, 37. https://doi.org/10.3389/fmicb.2012.00037
- Lovley, D.R., 2008. The microbe electric: conversion of organic matter to electricity. Curr. Opin. Biotechnol. 19, 564–571. https://doi.org/10.1016/j.copbio.2008.10.005
- Morgado, L., Paixão, V.B., Schiffer, M., Pokkuluri, P.R., Bruix, M., Salgueiro, C.A., 2012. Revealing the structural origin of the redox-Bohr effect: The first solution structure of a cytochrome from Geobacter sulfurreducens. Biochem. J. 441, 179–187. https://doi.org/10.1042/BJ20111103
- Paquete, C.M., Rusconi, G., Silva, A. V., Soares, R., Louro, R.O., 2019. A brief survey of the "cytochromome." Adv. Microb. Physiol. 75, 69–135. https://doi.org/10.1016/BS.AMPBS.2019.07.005
- Pous, N., Balaguer, M.D., Colprim, J., Puig, S., 2018. Opportunities for groundwater microbial electroremediation. Microb. Biotechnol. 11, 119–135. https://doi.org/10.1111/1751-7915.12866
- Pous, N., Carmona-Martínez, A.A., Vilajeliu-Pons, A., Fiset, E., Bañeras, L., Trably, E., Balaguer, M.D., Colprim, J., Bernet, N., Puig, S., 2016. Bidirectional microbial electron transfer: Switching an acetate oxidizing biofilm to nitrate reducing conditions. Biosens. Bioelectron. 75, 352–358. https://doi.org/10.1016/j.bios.2015.08.035
- Pous, N., Koch, C., Colprim, J., Puig, S., Harnisch, F., 2014. Extracellular electron transfer of biocathodes: Revealing the potentials for nitrate and nitrite reduction of denitrifying microbiomes dominated by Thiobacillus sp. Electrochem. commun. 49, 93–97. https://doi.org/10.1016/j.elecom.2014.10.011
- Pous, N., Puig, S., Balaguer, M.D., Colprim, J., 2017. Effect of hydraulic retention time and substrate availability in denitrifying bioelectrochemical systems. Environ. Sci. Water Res. Technol. 3, 922–929. https://doi.org/10.1039/c7ew00145b
- Pous, N., Puig, S., Dolors Balaguer, M., Colprim, J., 2015. Cathode potential and anode electron donor evaluation for a suitable treatment of nitrate-contaminated groundwater in bioelectrochemical systems. Chem. Eng. J. 263, 151–159. https://doi.org/10.1016/j.cej.2014.11.002
- Quejigo, J.R., Korth, B., Kuchenbuch, A., Harnisch, F., 2021. Redox Potential Heterogeneity in Fixed-Bed Electrodes Leads to Microbial Stratification and Inhomogeneous Performance. ChemSusChem 14, 1155–1165. https://doi.org/10.1002/cssc.202002611
- Quejigo, J.R., Rosa, L.F.M., Harnisch, F., 2018. Electrochemical characterization of bed electrodes using voltammetry of single granules. Electrochem. commun. 90, 78–82. https://doi.org/10.1016/j.elecom.2018.04.009
- Rosenbaum, M., Aulenta, F., Villano, M., Angenent, L.T., 2011. Cathodes as electron donors for microbial metabolism: Which extracellular electron transfer mechanisms are involved? Bioresour. Technol. 102, 324–333. https://doi.org/10.1016/j.biortech.2010.07.008
- Sevda, S., Sreekishnan, T.R., Pous, N., Puig, S., Pant, D., 2018. Bioelectroremediation of perchlorate and nitrate contaminated water: A review. Bioresour. Technol. 255, 331–339. https://doi.org/10.1016/j.biortech.2018.02.005
- Skiba, U., 2008. Denitrification, in: Jørgensen, S.E., Fath, B.D. (Eds.), Encyclopedia of Ecology. Academic Press, Oxford, pp. 866–871. https://doi.org/10.1016/B978-008045405-4.00264-0
- Twomey, K.M., Stillwell, A.S., Webber, M.E., 2010. The unintended energy impacts of increased nitrate

- contamination from biofuels production. J. Environ. Monit. 12, 218–224. https://doi.org/10.1039/b913137j
- Van Doan, T., Lee, T.K., Shukla, S.K., Tiedje, J.M., Park, J., 2013. Increased nitrous oxide accumulation by bioelectrochemical denitrification under autotrophic conditions: Kinetics and expression ofdenitrification pathway genes. Water Res. 47, 7087–7097. https://doi.org/10.1016/j.watres.2013.08.041
- Vilà-Rovira, A., Puig, S., Balaguer, M.D., Colprim, J., 2015. Anode hydrodynamics in bioelectrochemical systems. RSC Adv. 5, 78994–79000. https://doi.org/10.1039/c5ra11995b
- Vilar-Sanz, A., Pous, N., Puig, S., Balaguer, M.D., Colprim, J., Bañeras, L., 2018. Denitrifying nirK-containing alphaproteobacteria exhibit different electrode driven nitrite reduction capacities. Bioelectrochemistry 121, 74–83. https://doi.org/10.1016/j.bioelechem.2018.01.007
- Wang, K., Zhang, S., 2019. Extracellular electron transfer modes and rate-limiting steps in denitrifying biocathodes. Environ. Sci. Pollut. Res. 26, 16378–16387. https://doi.org/10.1007/s11356-019-05117-x
- Wang, X., Aulenta, F., Puig, S., Esteve-Núñez, A., He, Y., Mu, Y., Rabaey, K., 2020. Microbial electrochemistry for bioremediation. Environ. Sci. Ecotechnology 1, 100013. https://doi.org/10.1016/j.ese.2020.100013
- Xu, X., He, Q., Ma, G., Wang, H., Nirmalakhandan, N., Xu, P., 2018. Selective separation of mono- and divalent cations in electrodialysis during brackish water desalination: Bench and pilot-scale studies. Desalination 428, 146–160. https://doi.org/10.1016/J.DESAL.2017.11.015
- Zeppilli, M., Dell'Armi, E., Di Franca, M.L., Matturro, B., Feigl, V., Molnár, M., Berkl, Z., Németh, I., Rossetti, S., Papini, M.P., Majone, M., 2022. Evaluation of a Bioelectrochemical Reductive/Oxidative Sequential Process for Chlorinated Aliphatic Hydrocarbons (Cahs) Removal from a Real Contaminated Groundwater. SSRN Electron. J. 49, 103101. https://doi.org/10.2139/ssrn.3981653
- Zhang, X., Li, X., Zhao, X., Li, Y., 2019. Factors affecting the efficiency of a bioelectrochemical system: a review. RSC Adv. 9, 19748–19761. https://doi.org/10.1039/C9RA03605A
- Zhao, F., Xin, J., Yuan, M., Wang, L., Wang, X., 2022. A critical review of existing mechanisms and strategies to enhance N2 selectivity in groundwater nitrate reduction. Water Res. 209, 117889. https://doi.org/10.1016/j.watres.2021.117889
- Zhao, J., Li, F., Cao, Y., Zhang, X., Chen, T., Song, H., Wang, Z., 2021. Microbial extracellular electron transfer and strategies for engineering electroactive microorganisms. Biotechnol. Adv. 53, 107682. https://doi.org/10.1016/j.biotechadv.2020.107682
- Zhong, L., Yang, S.S., Ding, J., Wang, G.Y., Chen, C.X., Xie, G.J., Xu, W., Yuan, F., Ren, N.Q., 2021. Enhanced nitrogen removal in an electrochemically coupled biochar-amended constructed wetland microcosms: The interactive effects of biochar and electrochemistry. Sci. Total Environ. 789, 147761. https://doi.org/10.1016/J.SCITOTENV.2021.147761